International Journal of Nanomedicine

Dovepress
open access to scientific and medical research

Open Access Full Text Article

ORIGINAL RESEARCH

Inhibition of Ureteral Stricture by Pirfenidone-Loaded Nanoparticle-Coated Ureteral Stents with Slow-Release Pirfenidone

Zhaosheng Jiang[1,*], Jiahao Wang[2,*], Wei Meng[1,*], Youlang Zhou[3], Limin Ma[1], Yangbo Guan[1]

[1]Department of Urology, Affiliated Hospital of Nantong University, Medical School of Nantong University, Nantong, People's Republic of China; [2]Department of Urology, Wuxi Hospital Affiliated to the Nanjing University of Chinese Medicine, Wuxi, People's Republic of China; [3]Research Central of Clinical Medicine, Affiliated Hospital of Nantong University, Nantong, People's Republic of China

*These authors contributed equally to this work

Correspondence: Yangbo Guan; Limin Ma, Tel +86 18912888908; Tel +86 13404292020, Email guanyangbo123@ntu.edu.cn; ntmalimin@163.com

Introduction: Ureteral stricture caused by iatrogenic ureteral injury induced ureteral injury is more common and challenging to recover quickly. The effective prevention of ureteral stricture due to iatrogenic ureteral injury-induced ureteral damage is a current challenge for urologists. The purpose of this study was to evaluate the effectiveness of nanoparticle/pirfenidone complex-coated ureteral stents with slow-release pirfenidone for the prevention of ureteral stricture in rabbits. In this study, we developed a nanoparticle/pirfenidone complex-coated ureteral stent to deliver pirfenidone into the injured ureter to inhibit ureteral stricture.

Methods: Twelve New Zealand rabbits were divided into four groups: Sham, US, US+ Unmodified ureteral stent, and US+NP/PFD ureteral stent; we constructed an irreversible electroporation model of ureteral injury in rabbits and placed unmodified ureteral stents and nanoparticle/pirfenidone complex-coated ureteral stents into the ureter. Two weeks later, we euthanized the rabbits and removed their bilateral kidneys and ureters. We evaluated the effect of ureteral stent prophylaxis by gross specimen observation, section staining, and Western Blot.

Results: We found that the nanoparticle/pirfenidone complexes could adhere uniformly to the surface of the ureteral stent. After placement into the ureter, the nanoparticle/pirfenidone complexes were able to remain on the surface of the ureteral stent. We found nanoparticle/pirfenidone complexes could diffuse in the ureteral epithelial tissue two weeks after the order. The study showed that nanoparticle/pirfenidone complex-coated ureteral stents placed into the ureter showed significantly less stenosis due to fibrosis than in US control rabbits and rabbits treated with unmodified ureteral stents.

Conclusion: We used a novel platform based on nanoparticle/pirfenidone complex-coated ureteral stents for local and sustained delivery of pirfenidone, which can effectively deliver pirfenidone to the tissue and can slowly control the release of pirfenidone. Therefore, combining ureteral stents with nanoparticle/pirfenidone complexes was an effective measure to prevent ureteral stricture.

Keywords: nanoparticles, ureteral stricture, fibrosis, ureteral stents, pirfenidone

Introduction

Ureteral stricture is defined as functional obstruction due to ureteral stricture caused by various causes such as iatrogenic ureteral injury, stones, malignancy, inflammation, fibrosis, ischemia, and trauma.[1,2] In recent years, concomitant iatrogenic ureteral injury has been growing with the increasing use of Ureteroscopy techniques. The probability of medically induced ureteral injury is reported to be 60%-94% in China and abroad.[3,4] In particular, there is an increased rate of medically induced ureteral strictures due to the use of ureteroscopy for upper urinary tract stones.[5] Therefore, how to prevent ureteral strictures caused by iatrogenic ureteral injury, especially after ureteroscopic operations, is an urgent problem for urologists today.

Ureteral injury repair is usually a fibrous scar repair, characterized pathologically by massive fibroblast proliferation and excessive deposition of collagen and proteoglycans in the extracellular matrix, resulting in a disorganized collagen

Received: 20 September 2022
Accepted: 9 December 2022
Published: 21 December 2022

fiber arrangement. Studies have shown that TGF-β1 was highly expressed in fibroblasts and was the most closely related cytokine involved in scar production.[6,7] In this study, we attempted to further explore the mechanism of ureteral stricture by using an animal ureteral injury model to simulate the damage caused by medical endoscopic ureteral manipulation. Currently, the leading animal models of ureteral injury at home and abroad are the unilateral ureteral complete obstruction method and the electrocoagulation injury ureter method.[8] Therefore we attempted to explore the mechanism of ureteral stricture further using a model of ureteral injury in rabbits that more closely resembles the clinical ureteral stricture caused by ureteroscopic manipulation with electrocoagulation.

The essence of ureteral stricture prevention is the inhibition of fibroblast proliferation and transformation, the inhibition of extracellular matrix deposition and the expression of other fibrotic factors.[9] In recent years pirfenidone (PFD) has had a significant role in the antifibrotic treatment of various organs. It has been shown that the MAPK signaling pathway plays a vital role in the TGF-β1-induced transformation of epithelial cells into myofibroblasts, and pirfenidone can produce antifibrotic effects by antagonizing MAPK signaling pathway.[10,11] Therefore, in the present study, we chose PFD to inhibit the production of ureteral fibrous rings. How to deliver the PFD to the ureteral injury site is also a problem we need to address. We envisage that it allows the PFD to be loaded on the ureteral stent to act directly on the ureteral wall. However, when PFD is loaded now onto the ureteral stent, the PFD is susceptible to degradation by direct exposure to the tissue environment, and the lack of sustained release properties prevents continuous drug delivery, limiting the therapeutic effect. Therefore, finding a drug delivery system that can act consistently and controllably at the site of the lesion is essential.

In recent years, using nanoparticles as a carrier to treat diseases has become a new treatment modality. Nanoparticle drug delivery system with biodegradability and controlled release.[12] It has been found that nanoparticle sustained-release therapy is targeted and can continuously modulate the expression of drug retardation during the treatment process. Therefore, it has also gained more and more attention.[13,14] In recent years, polydopamine is a newly discovered bionic polymer that is the main component of mucin secreted by mussel proteins.[15] Studies have shown that dopamine can polymerize to form polydopamine when exposed to an alkaline environment.[16] PFD-loaded PLGA nanoparticles were then absorbed onto the ureteral stent surface by Van der Waals adsorption.[17]

The purpose of this study was to explore the effectiveness of nanoparticle/pirfenidone complex-coated ureteral stents in inhibiting ureteral stricture. We have innovatively developed a nanoparticle/pirfenidone complex-coated ureteral stent and investigated its morphological characteristics, biocompatibility, and release capacity. We also evaluated the effect of the drug-laden stent on the inhibition of ureteral stricture by observing large specimens, section staining, and Western Blot using an animal model of electrocoagulation ureter.

Material and Methods

Preparation of Nanoparticle/PFD Complexes

In this study, the nanoparticles were obtained using a double emulsion method, similar to previous studies.[18–20] Briefly, 200ul of phosphate-buffered saline (PBS), including PFD, was emulsified in 4mL of dichloromethane, including 40mg of poly (lactic-co-glycolic acid) (PLGA, Mw=40,000–75,000, Sigma. Saint Louis, USA) using a Sonoplus HD 2070 Ultrasonic homogenizer (Bandelin electronic, Berlin, Germany) for 1 min over an ice bath. Then, add 9mL of 1.5% poly (vinyl alcohol) (PVA; Mw=14,160) to the mixture to form the double emulsion. Next, the emulsion was re-emulsified by sonication on an ice bath for 3 minutes and then stirred at room temperature for 24 hours to evaporate the dichloromethane completely. The nanoparticles were centrifuged for 5 minutes at 12,000 RPM below 4°C. Finally, the nanoparticles were washed three times with deionized water and suspended in deionized water.

Preparation and Characterization of Nanoparticle/Pirfenidone Complex-Coated Ureteral Stents

The ureteral stent (Fr3L, 120mm, China) was modified with polydopamine. These ureteral stents were first incubated in phosphate buffer solution (PBS) (5 Mm, PH8.5) containing dopamine hydrochloride (0.5mg/mL). Next, the polydopamine-modified ureteral stents were formed by stirring for 3 hours at room temperature. The polydopamine-modified

ureteral stents were washed twice with deionized water and then immersed in the previously prepared PFD-loaded nanoparticles suspension to form PFD-loaded nanoparticles-coated ureteral stents. Scanning electron microscopy (SEM, Hitachi, S-3400N, Tokyo, Japan) was used to observe the surface morphology of ureteral stents coated with nanoparticles.

Preparation of Rhodamine B Labeled Nanoparticle/Pirfenidone Complexes

In order to confirm the distribution of nanoparticles after the insertion of PFD-loaded nanoparticles coated ureteral stents into the ureter. We used Rhodamine B (Sigma-Aldrich) to label nanoparticle/pirfenidone complexes. Firstly, Rhodamine B-loaded nanoparticles were prepared in the same way as above. 100ul of phosphate-buffered saline (PBS), including Rhodamine B, was emulsified in 2mL of dichloromethane, including 20mg of PLGA, by sonication for 0.5 min over an ice bath. Then, add 4.5mL of 1.5% PVA to the mixture to form the double emulsion. Next, the emulsion was re-emulsified by sonication on an ice bath for 3 minutes and then stirred at room temperature for 24 hours to completely evaporate the dichloromethane. The nanoparticles were centrifuged for 5 minutes at 12,000 RPM below 4°C. Finally, the nanoparticles were washed three times with deionized water and suspended in deionized water.

Preparation of Rhodamine B Loaded Nanoparticles-Coated Ureteral Stents

These ureteral stents were firstly incubated in phosphate buffer solution (PBS) (5 Mm, PH8.5) containing dopamine hydrochloride (0.5mg/mL) and following the polydopamine-modified ureteral stents were formed by stirring for 3 hours at room temperature. The polydopamine-modified ureteral stents were washed twice with deionized water and then immersed in the previously prepared Rhodamine B-loaded nanoparticles suspension to form Rhodamine B-loaded nanoparticles-coated ureteral stents.

Release in vitro

The amount of PFD released from the nanoparticles-coated ureteral stent was measured in a PBS buffer solution (pH 7.4). A 30mm long ureteral stent was incubated in 2mL of PBS, including 0.02% w/v sodium azide, and placed in a 37°C constant temperature incubator. We changed the buffer on day 1, day 3, day 7, day 14, day 21, and day 28; respectively, 2mL of fresh PBS buffer was replaced with 2mL of the removed release solution. The collected key was stored at −80°C, after which the amount of released PFD was determined using an enzyme-linked immunosorbent assay (BioOcean, Shoreview, MN). The experiment was performed in triplicate.

Cytotoxicity of Nanoparticle/Pirfenidone Complex-Coated Ureteral Stents

The cytotoxicity of nanoparticle/pirfenidone complex-coated ureteral stents was using the CCK8 assay. In short, 20mm long sterile ureteral stents were cut into 2mm lengths and placed into a 96-well plate. Next, cell suspension (SV-HUC-1, PC101) was added to a 96-well (0.5×10^4 cells/well). After 24 and 48 h of incubation, 10 μL of the CCK8 dye solution (10 mg/mL, Sigma) was added to the medium in each well and continued to culture for 4 hours in the incubator at 37°C under an atmosphere of 5% CO2. The absorbance values of each well were measured at 450nm using a microplate reader. Untreated cells were taken as control with 100% viability. The experiment was performed in triplicate.

An Experimental Model of Injured Ureteral

Twelve male New Zealand rabbits, aged 20 weeks, were used as experimental models. The Experimental Animal Care and Committee approved the animal experiments of Nantong University (Approval No. S20210301-991). The welfare of the laboratory animals followed《GB/T 35892–2018》. Twelve New Zealand rabbits were divided into four groups: Sham, US, US +Unmodified ureteral stent, and US+NP/PFD ureteral stent. All rabbits were injected intramuscularly with Sumianxin II (1mL/kg) + Zoletil 50 (0.4mL/kg). After general anesthesia, the rabbit was fixed supine on the operating table Take the middle abdominal incision, cut the skin, subcutaneous tissue, and rectus abdominis muscle layer by layer, open the peritoneum and enter the abdominal cavity. After entering the abdominal cavity, the descending colon and small intestine mesentery were pushed apart, the adipose tissue was bluntly separated, and a section of the ureter about 1 cm long was freed. The electrocoagulation guidewire (LK-3, China) was inserted into the ureter, and the ureter was

electrocautery with 10w electrocoagulation for 2 seconds, and the guidewire was withdrawn. Closure of the abdominal cavity after consolidation and retraction of the small intestine. Three days after surgery, daily cephalosporin intramuscular injection to prevent infection.

In the treatment group, the ureter was successfully freed. A longitudinal incision was made in the middle of the ureter to place an unmodified ureteral stent and an NP/PFD ureteral stent, respectively, which were then damaged by electrocoagulation. The animals were euthanized two weeks after surgery, and the affected ureteral stricture and the treated segment (about 1 cm) were taken to compare the ureteral pathological changes and cytokine expression.

Histopathology and Immunohistochemical Staining Analysis

Two weeks after the ureteral injury and the ureteral stent placement, three rabbits in each group were killed by air embolism. Then bilateral ureter and kidneys of all rabbits were excised. The tissue was stored in a 10% formalin solution. The specimens were dehydrated, embedded in paraffin, and cut into 5μm thick sections. Staining slides with hematoxylin-eosin (H&E) and observing the changes in ureteral endothelial and lumen areas.

Immunohistochemistry was performed to detect the expression levels of TGF-β1 in the ureter. The slides were incubated with 3% hydrogen peroxide at room temperature for 5–10 min to block endogenous peroxidase activity. The water bath was set to 100°C; the slides were placed in citrate buffer (Dako, Glostrup, Denmark) solution for 5 min for antigen repair. The slides were washed three times with PBS for 5 min each and blocked with 5% BSA for two hours. The slides were then incubated with a rabbit anti-TGF beta 1 antibody (1:500, 21898-1-AP, proteintech) at 4°C overnight. Next, the slides were washed with PBS and incubated with a secondary antibody for 1 hour. The slides were stained with DAB for a color development and then counterstained with hematoxylin. The slides were then sealed with neutral gum, and a microscope (Leica DMR 3000, Leica Microsystems, Bensheim, Germany) was used to observe and evaluate tissue images.

Western Blot Analysis

The total protein from the ureteral tissues of the Sham, US, US+ Ureteral stent and US+ NP/PFD ureteral stent groups were extracted for Western blot analysis. The protein samples were separated on SDS-PAGE gels and transferred to polyvinylidene fluoride (PVDF) membranes. Then the membranes were washed with TBST buffer (50 mm Tris-HCL, 100mm NaCl, and 0.1% Tween-20, pH7.6) and blocked for 2 hours with 5% skimmed dry milk in TBST. Next, the membranes were incubated overnight at 4°C with a rabbit anti-TGF beta 1 antibody (1:1000, 21898-1-AP, proteintech), a rabbit anti- Collagen Type I antibody (1:2000, GB114197, servicebio), and a rabbit anti-Collagen Type III antibody (1:1000, GB111323, servicebio). All experiments were repeated three times. The next day, primary antibodies were decanted, and the membranes were washed three times with TBST at room temperature for 10min and then incubated with secondary antibody at 4°C overnight. The way of washing the membrane is the same as above, and then the Odyssey infrared imaging system (LI-COR, Lincoln, NE, USA) was used to visualize the protein bands. The expression of each protein band was determined using ImageJ software, and the expression of the protein bands was normalized to that of GAPDH.

Statistical Analysis

All values were expressed as the mean ± standard deviation (SD). An unpaired *t*-test was used to test for difference between groups. The difference among the three groups was analyzed by one-way variance analysis (ANOVA) with GraphPad Prism 9 software. P values <0.05 were considered statistically significant.

Results

Characterization and Evaluation of Nanoparticle/Pirfenidone Complex-Coated Ureteral Stents

In order to load PFD on the surface of ureteral stents, we first encapsulated PFD in the nanoparticles. The nanoparticles have two advantages; one has a slow-release capability, and the other can keep PFD from degradation and denaturation.

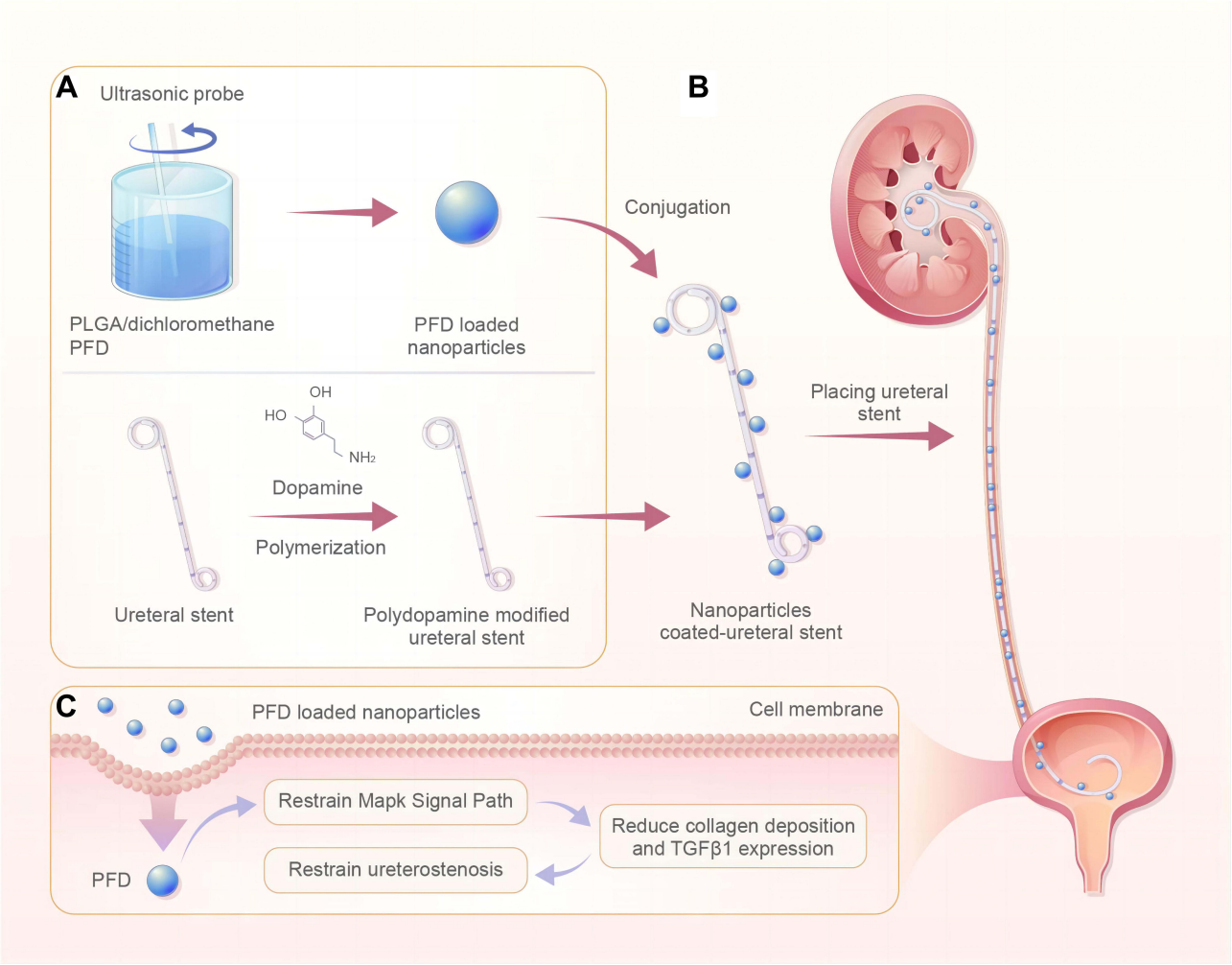

Figure 1 Schematic diagram of the process of preparing a nanoparticle/ pirfenidone complex-coated ureteral stents for restraining ureter stenosis. (**A**) Preparation of nanoparticle/pirfenidone complex-coated ureteral stents. (**B**) Placement of the modified ureteral stent into the ureter. (**C**) Nanoparticles release PFD to relieve ureter stenosis.

The ureteral stents were then placed in a solution containing dopamine to form a layer of adhesive polydopamine. Next, the polydopamine-modified ureteral stents were placed in a suspension containing nanoparticles/PFD complexes to allow the ureteral stents' surface to be loaded with nanoparticles/PFD complexes. Finally, the nanoparticle/PFD complex-coated ureteral stents were prepared and used to prevent ureteral stricture, as shown in Figure 1.

In this study in order to confirm whether nanoparticles/PFD complexes are wrapped on the surface of the ureteral stents and the distribution of nanoparticles/PFD complexes on the surface of the ureteral stents. We use SEM to observe the nanoparticles/PFD complexes that can be coated on the surface of the ureteral stents. In addition, we also detected whether a large amount of nanoparticles/PFD complexes on the surface of ureteral stents fell off after ureter placement. We found that many nanoparticles/PFD complexes remained on the surface of the stent after ureter placement. Figure 2 represents the ureteral stent's representative SEM images in three different states (Unmodified ureteral stent, NP/PFD coated ureteral stents, NP/PFD coated ureteral stents after friction). These SME images suggest that large amounts of nanoparticles/PFD complexes remain on the surface of the stent even after ureter placement.

Distribution of Nanoparticles/PFD Complexes in the Ureter

One week after Rhodamine B loaded nanoparticles-coated ureteral stent implantation, we found a large amount of red fluorescence around the ureter tissue, indicating that nanoparticles/PFD complexes on the stent could be shed and

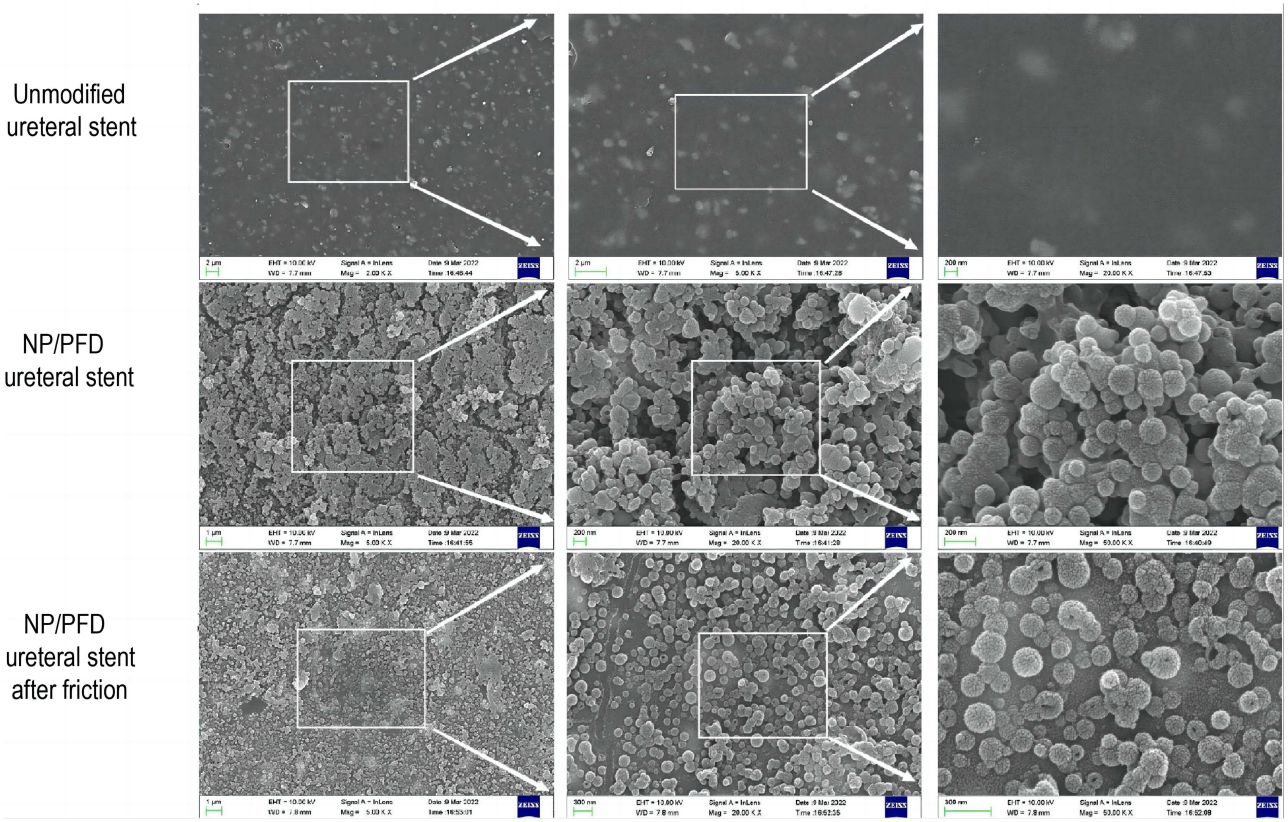

Figure 2 Typical scanning electron microscopy images of ureteral stents. Scanning electron microscopy images of ureteral stents under different conditions (unmodified ureteral stent, nanoparticle/pirfenidone complex-coated ureteral stents, and nanoparticle/pirfenidone complex-coated ureteral stents after friction).

diffused into the surrounding tissue. Figure 3 showed a fluorescent image of an unmodified ureteral stent; we found no red fluorescent around the ureter tissue. Meanwhile, in a fluorescent image of PFD-loaded nanoparticles ureteral stent, we discovered red fluorescent around the ureter tissue.

In vitro Release

Continued release of PFD is significant to prevent ureteral stricture. Therefore, we chose a degradable polylactic-co-glycolic acid (PLGA) to synthesize nanoparticles. The diameter of these nanoparticles/PFD complexes was further tested by dynamic light scattering (DLS), and the average diameter of the complexes was 142±39.91nm (Figure 4A). Figure 4B shows the in vitro release profiles of PFD-loaded nanoparticles coated ureteral stents. Within the first three days, we found that approximately 20% of the PFD could be released from the nanoparticles-coated ureteral stents. Finally, about 80% of the PFD was released slowly and continuously from the nanoparticles within 30 days. These results indicate that the sustained release of PFD can be achieved by using nanoparticles-coated ureteral stents.

Cytotoxicity of the Nanoparticle/PFD Complex-Coated Ureteral Stents

In order to evaluate the biotoxicity of the nanoparticle/PFD complex-coated ureteral stents, the cytotoxicity of nanoparticle/PFD complex-coated ureteral stents on human ureteral epithelial cells cultured in vitro was determined by CCK8 assay. We found that unmodified ureteral stents, nanoparticles, and nanoparticle/PFD complex-coated ureteral stents had no significant cytotoxicity after 24 h and 48 h of coculture compared with untreated cultured cells (Figure 4C and D).

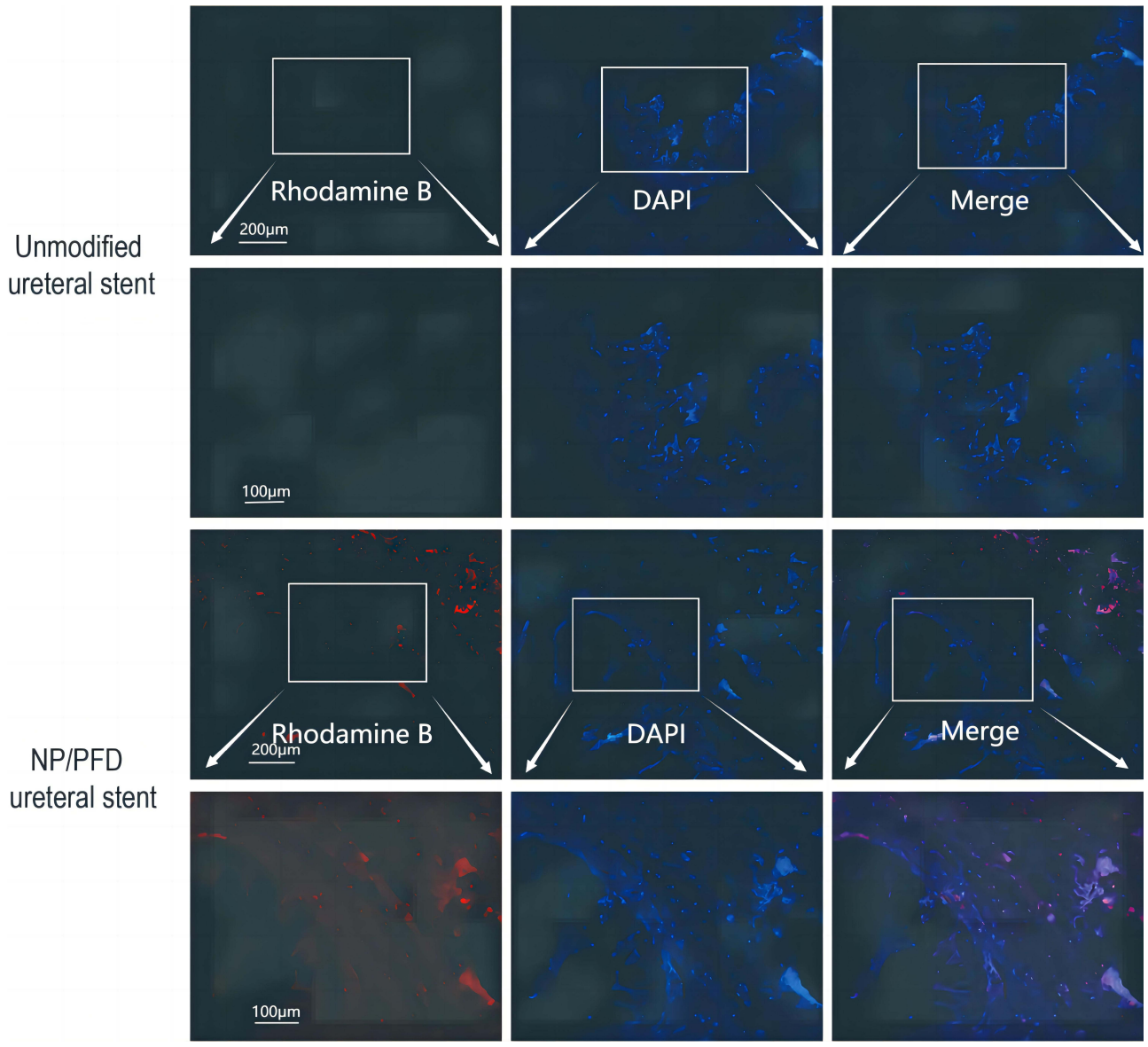

Figure 3 The distribution of the nanoparticles in ureteral tissue after placement of nanoparticle/pirfenidone complex-coated ureteral stents into the ureter. One week after placement, the distribution of Rhodamine B labeled unmodified ureteral stents and nanoparticle/pirfenidone complexes in ureteral tissue.

In vivo Rabbit Ureter Heat Injury Model and Gross Specimen Changes

Figures 5A and B show the rabbit ureteral electrical injury model and the electrical injury model after ureteral stent placement. Two weeks later, we euthanized the rabbits and removed their bilateral kidneys and ureters. The changes in the gross specimens of the kidney and ureter of rabbits are shown in Figure 6.

Hematoxylin and Eosin and Immunohistochemical Staining Analysis

As shown in Figure 7A, HE staining of the ureteral cross-section in the US group showed severe stenosis in the rabbit ureter. Meanwhile, the ureteral stricture was somewhat improved with the placement of unmodified ureteral stents, while the stenosis was significantly enhanced with the placement of the nanoparticles-coated ureteral stents. Figure 7B shows the quantification of the ureteral lumen area for each group. Figure 8 shows the difference in the positive expression of TGF-β1 between the different groups by IHC.

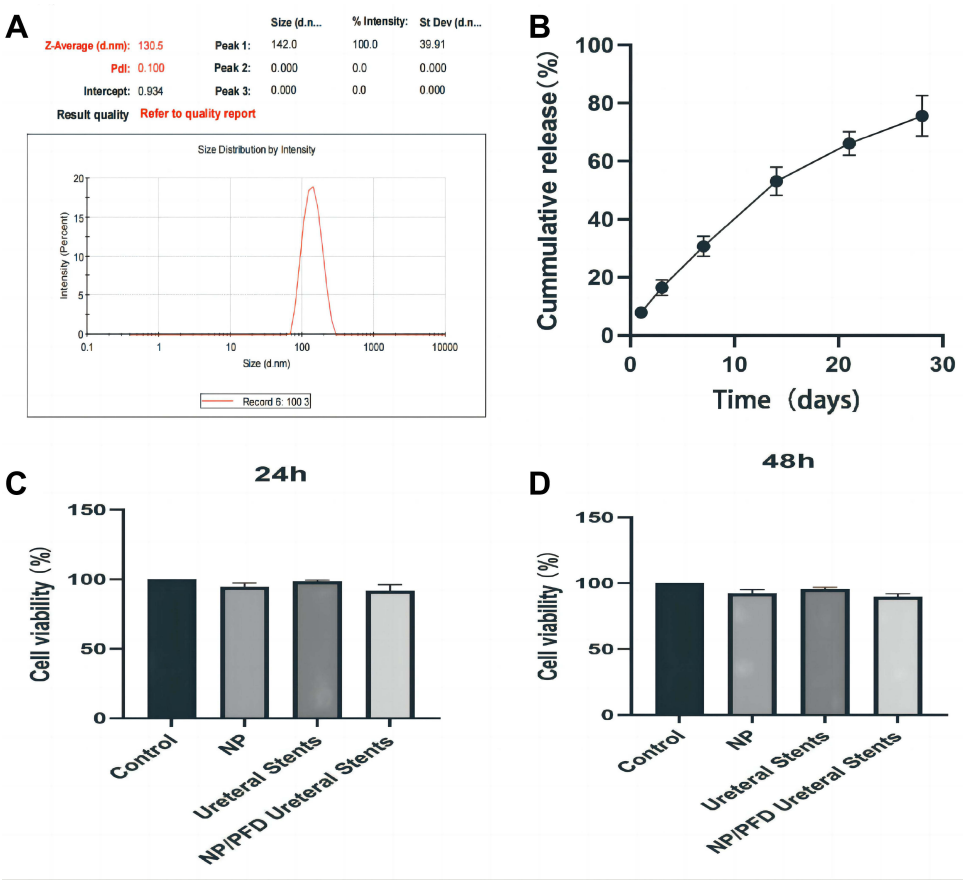

Figure 4 Characteristics of nanoparticle/pirfenidone complex-coated ureteral stents. (**A**) Hydrodynamic diameter distributions of the nanoparticles/PFD complexes. (**B**) In vitro release profiles of PFD from nanoparticles coated ureteral stents in PBS with pH 7.4. (**C** and **D**) In vitro cytotoxicity of different ureteral stents and nanoparticles on ureteral endothelial cells after 24 and 48 hours of incubation. Compared to the control group, ureteral stents, nanoparticles, and NP/PFD ureteral stents had no significant effect on cell viability.

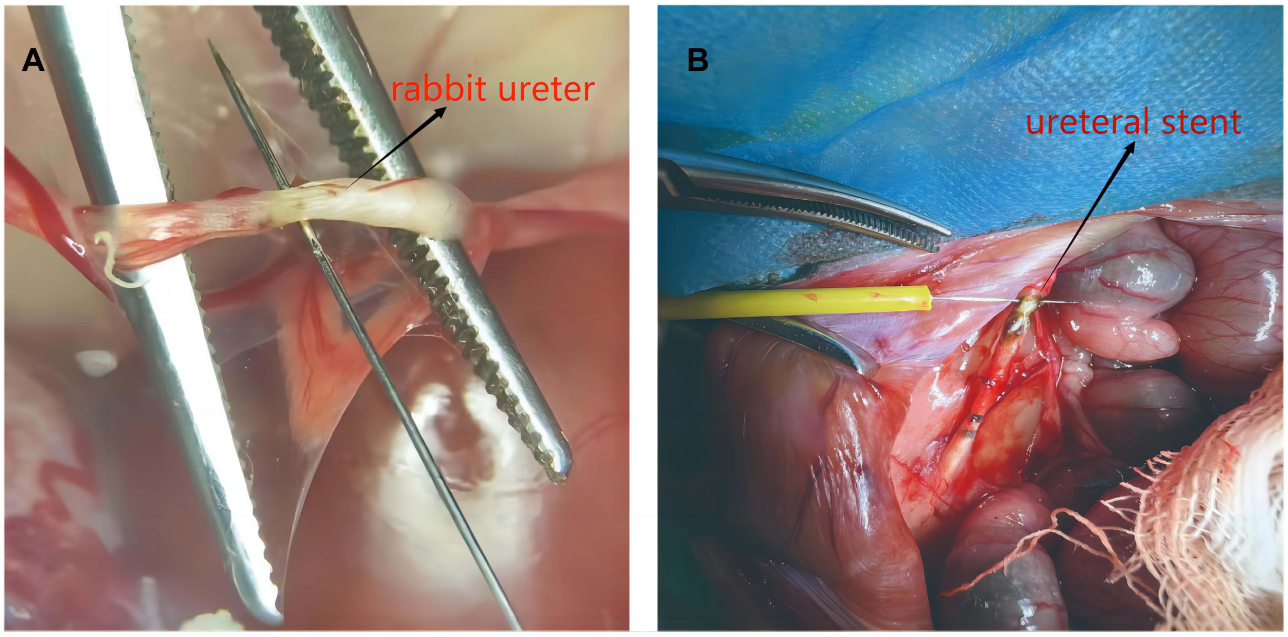

Figure 5 Rabbit ureteral electric injury model and ureteral stent placement. (**A**) A one-centimeter-long segment of the ureter with heat injury was created by using an electrocoagulation device. (**B**) We placed the unmodified stent and nanoparticle/pirfenidone complex-coated ureteral stents. Into the ureter separately, and then performed electrical damage on the ureter.

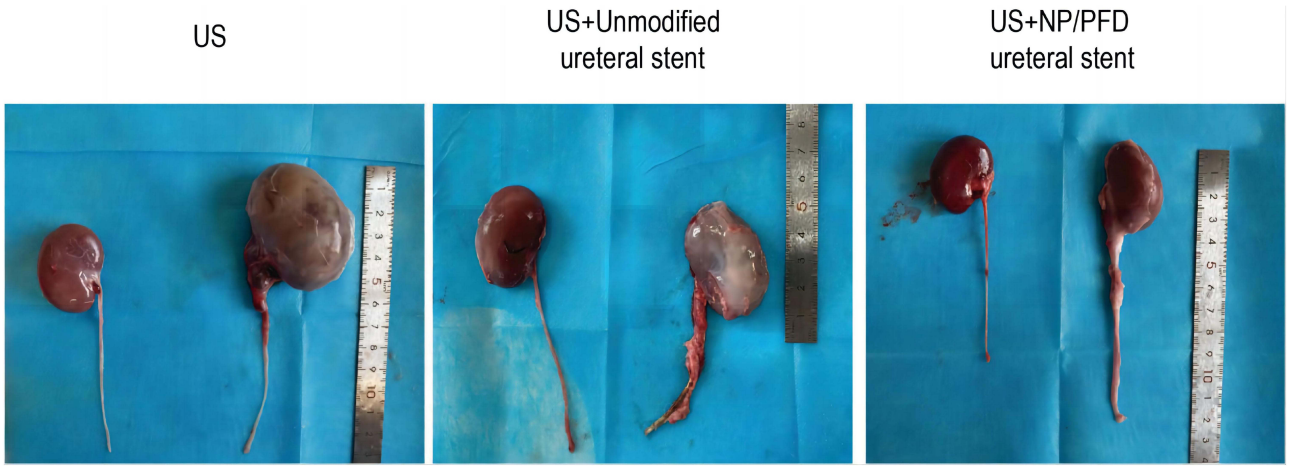

Figure 6 Gross appearance of the kidney and ureter after 2 weeks. The degree of hydronephrosis and ureteral obstruction in the US+NP/PFD ureteral stent and US +Unmodified ureteral stent group was significantly smaller than that in the US group. There is no significant difference between the US +NP/PFD ureteral stent and US +Unmodified ureteral stent.

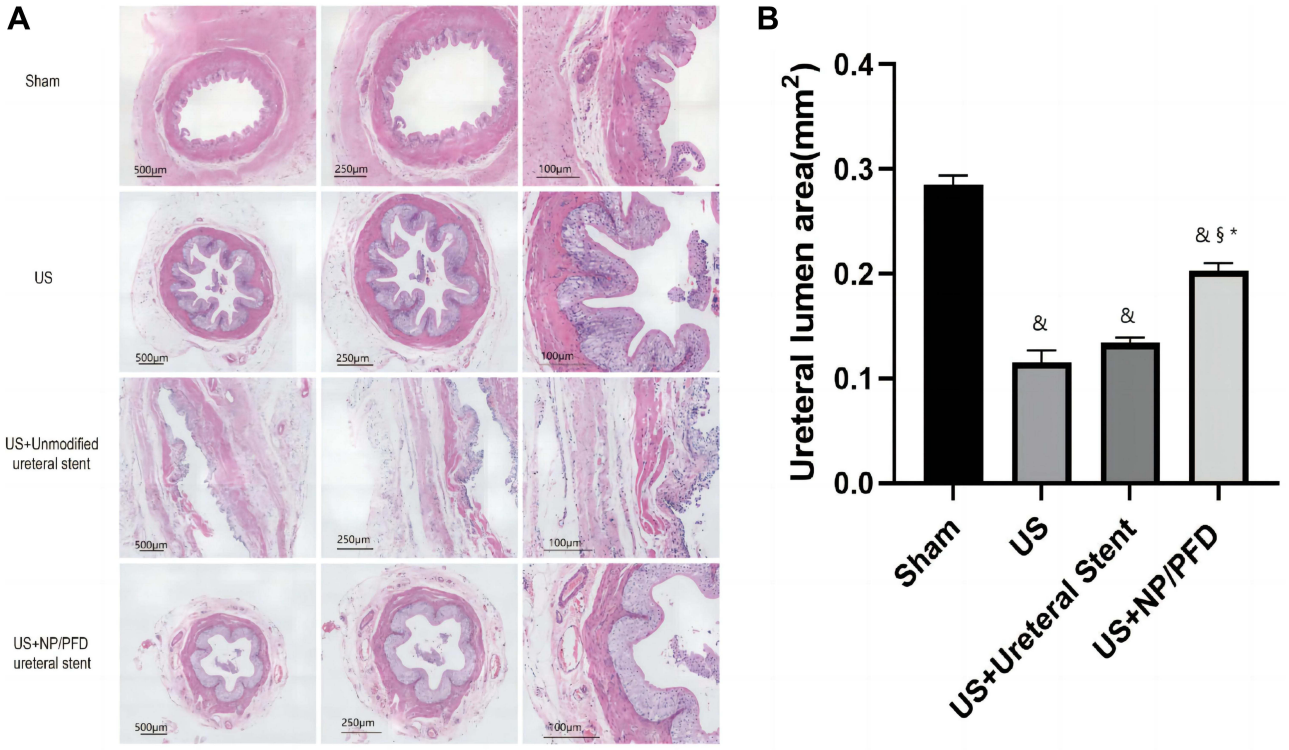

Figure 7 Micrographs of hematoxylin staining. (**A**) The ureteral lumen was significantly narrower in the US group, and the diameter of the ureteral lumen was larger in the US+NP/PFD ureteral stent group than in the other two groups. (**B**) The quantifications of ureteral lumen area for each group. [&]P<0.01 vs the Sham group. [§]P<0.01 vs the US group. *P<0.01 vs the US +Unmodified ureteral stent.

Western Blot Analysis Results

As shown in Figure 9, the protein expression levels of TGF-β1, COI I, and COI III were significantly higher in the US group than in the Sham group, unmodified ureteral stents and nanoparticles-coated ureteral stents (P<0.05). We can also find in the figure that the US+NP/PFD ureteral stent group is significantly better than the US and US+ Unmodified ureteral stent (P<0.05), and there is no significant difference between the US and US+ Unmodified ureteral stent (P>0.05).

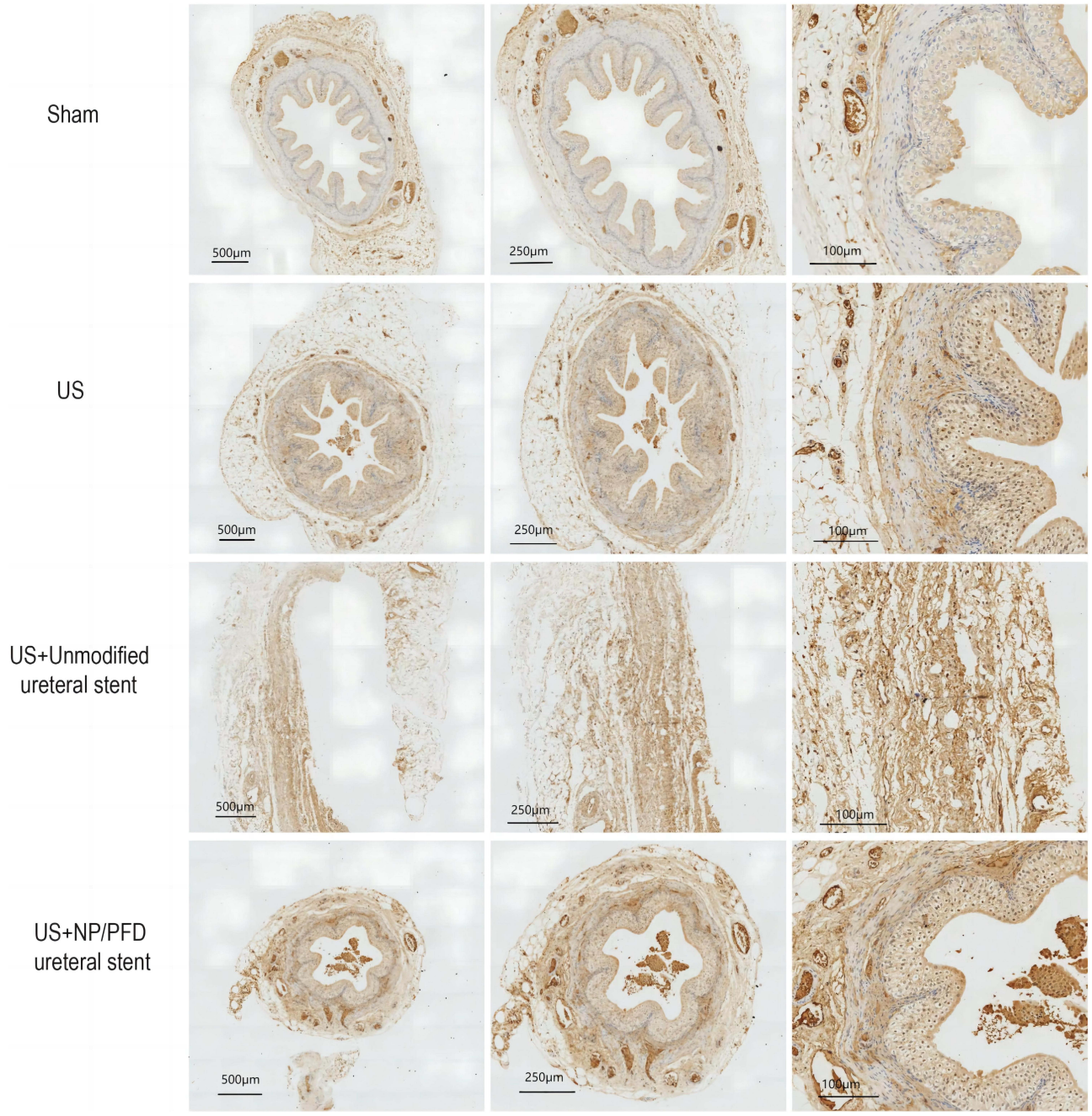

Figure 8 Micrographs of immunohistochemistry staining. The positive expression of TGFβ-1 in the US+NP/PFD ureteral stent group was lower than that in the US and US+ unmodified ureteral stent groups.

Discussion

Ureteral strictures are most often the result of medical manipulation.[21] With the continuous use of minimally invasive techniques in the field of surgery, the incidence of stenosis after a ureteral injury caused by some minimally invasive devices is increasing yearly, and the treatment outcome is poor. Therefore, it is of great clinical importance to study the prevention and treatment of stenosis after ureteral injury.

Ureteral stenting is currently one of the most common interventions to prevent and relieve ureteral stricture.[22] In this study, we worked on how to alleviate better ureteral strictures caused by medically induced manipulations. Several researchers have reported investigations on ureteral stents with rapamycin inhibitor elution, paclitaxel-coated stents, bone

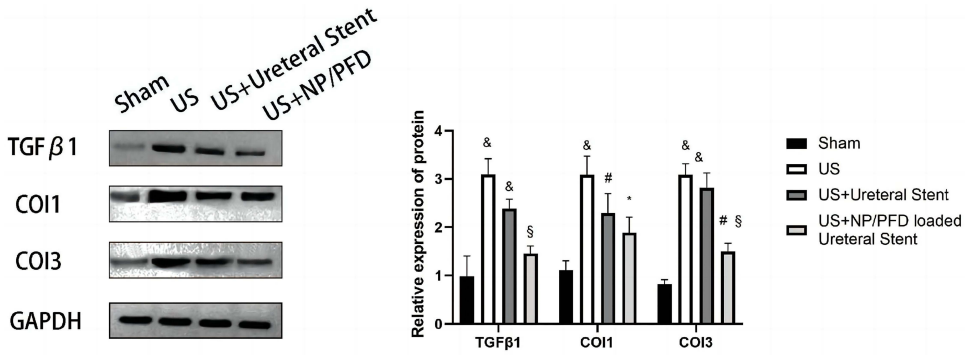

Figure 9 Western blot assay of ureter-related protein expression in each group. $^{\#}P < 0.05$ vs the Sham group, $^{\&}P < 0.01$ vs the Sham group, $^{*}P < 0.05$ vs the US group, $^{\S}P < 0.01$ vs the US group.

marrow mesenchymal stem cells, and biodegradable stents in the prevention and treatment of ureteral stricture.[23–26] However, these treatments are only in the research stage and have not yet been applied in the clinic, and the efficacy of these drugs in the ureter deserves further study. Therefore, based on these previous studies, we tried to find a new one that could better combine the drug with the ureteral stent and simultaneously deliver the drug to the ureter accurately.

In recent years, nanoparticles have been used as carriers in treating various diseases because of their biodegradable and slow-release advantages.[27] It was found that nanoparticles, with a diameter of less than 100 nm, can carry multiple drugs or genes and easily penetrate cell membranes.[28,29] In this study, we used rabbits as an animal model. Rabbits' urine composition differs greatly from that of human beings and may negatively affect stent assessment in this species. To solve this problem, we must ensure that the drug is not degraded by urine. To achieve this effect, we first encapsulated PFD in PLGA nanoparticles with good biocompatibility and slow-release ability, then wrapped the nanoparticles/PFD complexes in a polydopamine-modified ureteral stent, and finally placed the ureteral stent into the rabbit ureter to prevent and alleviate the occurrence of ureteral stricture (Figure 1). To confirm that the nanoparticles/PFD complexes can adhere uniformly to the surface of the ureteral stent, we observed a large number of nanoparticles/PFD complexes adhering uniformly to the surface of the stent by scanning electron microscopy. We also observed that a large number of nanoparticles/PFD complexes remained on the surface of the ureteral stent after placement into the ureter, which is the key to the successful delivery of nanoparticles to the tissue (Figure 2). In this study, we found that nanoparticles containing PFD could be efficiently delivered to tissues (Figure 3) and that the nanoparticles could release PFD slowly and efficiently over a period of one month (Figure 4B). The ultimate goal of this modified ureteral stent is to be used clinically, so it must have low biotoxicity and good biocompatibility. Our study found that the viability of urothelium was not significantly affected when co-cultured with nanoparticles, nanoparticle/PFD complex-coated ureteral stents, and plain ureteral stents (Figure 4C and D). This also lays a solid foundation for follow-up studies and future clinical applications.

In this study, we developed a similar model of electrical ureteral injury in rabbits based on the survey by Anidjar et al for the construction of a porcine ureteral stricture model.[30] The advantage of this modeling approach is that the degree of damage can be controlled and adjusted to simulate better ureteral strictures caused by medical manipulation in clinical practice. We used an electrocoagulation device to perform a penetrating injury to the rabbit ureter. In clinical practice, stents are placed at the end of the procedure. In this study, we initially attempted to perform electrocoagulation injury on the ureter first and then place the ureter. However, we found that the ureter was severely wrinkled after electrocoagulation injury, and forced placement may cause irreversible damage to the ureter. Our aim in this study was to inhibit the formation of stenosis after ureteral electrocoagulation injury, so we tried to place a drug-laden stent tube followed by electrocoagulation injury. Two weeks later, we removed the rabbit kidney and ureter specimens. We found that the degree of hydronephrosis and ureteral dilatation in the kidney with nanoparticles/PFD complex-coated ureteral stent were significantly lower than those in the molded and unmodified stent tube groups (Figure 6). We found by HE staining that the ureteral lumen was a significant narrowed considerably modeling group. The lumen was significantly dilated

after nanoparticles/PFD complex-coated ureteral stent treatment, and we can see the difference in the positive expression of TGF-β1 between the different groups by IHC (Figures 7 and 8). At the same time, we extracted proteins from the ureters of the four groups. We found that the expression of TGFβ-1, COI I, and COI III in the nanoparticles/PFD complex-coated ureteral stent group was significantly lower than that in the US group and unmodified group by Western blot. At the same time, there was no significant difference between the unmodified ureteral stent and the US group (Figure 9). Our study found that even though the ureter was placed first and electrocoagulation injury was performed later, it was effective in inhibiting the occurrence of stenosis.

In previous experimental studies, TGFβ-1 has been shown to play an essential role in ureteral fibrosis and stenosis.[31] Our analysis also confirmed that PFD released from nanoparticles attenuated the expression of TGFβ-1 and collagen deposition and reduced the extent of ureteral stricture. This provides a solid foundation for more in-depth research as well as clinical applications in the future. In many patients, ureteral stents were placed after the ureteral injury occurred, and the ureter was dilated to some extent. Still, fibrosis formation was not inhibited, leading to stenosis after stent removal. Nanoparticles/PFD complex-coated ureteral stents not only dilate the ureter but also fundamentally impede the formation of ureteral fibrosis, which can more effectively prevent ureteral stricture.

Our study also has some flaws. We chose two weeks for our research based on the survey by Dongshan Zhang et al.[32] We did not compare the fibrosis produced in the ureter at different time periods, and also our sample size was not large enough. Therefore, our future study will increase the sample size and also research the effect of prevention at different time periods after ureteral injury.

Conclusion

This study demonstrated that nanoparticles/PFD complex-coated ureteral stents could inhibit ureteral stricture by reducing TGFβ-1 expression and collagen deposition. Therefore, we believe that using nanoparticles/PFD complex-coated ureteral stents effectively prevents ureteral strictures caused by medical manipulation. However, since the experimental animals are rabbits, further research is needed for clinical application in the future.

Abbreviations

US, ureteral stricture; PFD, pirfenidone; TGF-β1, TGF beta 1; COI I, Collagen Type I; COI III, Collagen Type III; PLGA, polylactic-co-glycolic acid; DAB, NovolinkTM Polymer Detection System; NP/PFD, nanoparticle/PFD complexes.

Funding

This article was funded by the National Natural Science Foundation of China [grant number: 81771571] and the Science and Technology Project of Nantong, Jiangsu Province (No. MS12017006-4). The funder had no role in the study design, analysis, interpretation of data, the writing of the manuscript, and the decision to submit the article for publication.

Disclosure

The authors declare that there is no conflict of interest for the publication of this study.

References

1. Rotariu P, Yohannes P, Alexianu M., et al. Management of malignant extrinsic compression of the ureter by simultaneous placement of two ipsilateral ureteral stents. *J Endourol*. 2001;15(10):979–983. doi:10.1089/089277901317203047
2. Demanes D, Banerjee R, Cahan B, et al. Ureteral stent insertion for gynecologic interstitial high-dose-rate brachytherapy. *Brachytherapy*. 2015;14(2):245–251. doi:10.1016/j.brachy.2014.11.013
3. Aghaji A, Odoemene C. Ureteric injuries in Enugu, Nigeria. *East Af Med J*. 1999;76(4):184–188.
4. Rao D, Yu H, Zhu H, Duan P. The diagnosis and treatment of iatrogenic ureteral and bladder injury caused by traditional gynaecology and obstetrics operation. *Arch Gynecol Obstetrics*. 2012;285(3):763–765. doi:10.1007/s00404-011-2075-7
5. Delvecchio F, Auge B, Brizuela R, et al. Assessment of stricture formation with the ureteral access sheath. *Urology*. 2003;61(3):518–522. doi:10.1016/s0090-4295(02)02433-0
6. Kim K, Kim H, Hwang M, et al. The antifibrotic effect of TGF-beta1 siRNAs in murine model of liver cirrhosis. *Biochem Biophys Res Commun*. 2006;343(4):1072–1078. doi:10.1016/j.bbrc.2006.03.087

7. Zhang Z, Li X, Liu Y, Zhang X, Li Y, Xu W-S. Recombinant human decorin inhibits cell proliferation and downregulates TGF-beta1 production in hypertrophic scar fibroblasts. *J Int Soc Burn Injuries*. 2007;33(5):634–641. doi:10.1016/j.burns.2006.08.018
8. Xavier S, Vasko R, Matsumoto K, et al. Curtailing endothelial TGF-β signaling is sufficient to reduce endothelial-mesenchymal transition and fibrosis in CKD. *J Am Soc Nephrol*. 2015;26(4):817–829. doi:10.1681/asn.2013101137
9. Boehme S, Franz-Bacon K, DiTirro D, Ly T, Bacon KB. MAP3K19 Is a Novel Regulator of TGF-β Signaling That Impacts Bleomycin-Induced Lung Injury and Pulmonary Fibrosis. *PLoS One*. 2016;11(5):e0154874. doi:10.1371/journal.pone.0154874
10. Rhyu D, Yang Y, Ha H, et al. Role of reactive oxygen species in TGF-beta1-induced mitogen-activated protein kinase activation and epithelial-mesenchymal transition in renal tubular epithelial cells. *J Am Soc Nephrol*. 2005;16(3):667–675. doi:10.1681/asn.2004050425
11. Santibañez J. JNK mediates TGF-beta1-induced epithelial mesenchymal transdifferentiation of mouse transformed keratinocytes. *FEBS Lett*. 2006;580(22):5385–5391. doi:10.1016/j.febslet.2006.09.003
12. Chung Y, Hsieh W, Young T. Polycation/DNA complexes coated with oligonucleotides for gene delivery. *Biomaterials*. 2010;31(14):4194–4203. doi:10.1016/j.biomaterials.2010.01.116
13. Bolt P, Clerk AN, Luu HH, et al. BMP-14 Gene Therapy Increases Tendon Tensile Strength in a Rat Model of Achilles Tendon Injury. *JBJS*. 2007;89(6):1315–1320. doi:10.2106/jbjs.F.00257
14. Wong S, Argyros O, Harbottle R. Vector systems for prenatal gene therapy: principles of non-viral vector design and production. *Methods Mol Biol*. 2012;891:133–167. doi:10.1007/978-1-61779-873-3_7
15. Yang Z, Tu Q, Zhu Y, et al. Mussel-inspired coating of polydopamine directs endothelial and smooth muscle cell fate for re-endothelialization of vascular devices. *Adv Healthcare Materials*. 2012;1(5):548–559. doi:10.1002/adhm.201200073
16. Park J, Brust T, Lee H, Lee S, Watts V, Yeo Y. Polydopamine-based simple and versatile surface modification of polymeric nano drug carriers. *ACS Nano*. 2014;8(4):3347–3356. doi:10.1021/nn405809c
17. Wei P, Xu Y, Gu Y, Yao Q, Li J, Wang L. IGF-1-releasing PLGA nanoparticles modified 3D printed PCL scaffolds for cartilage tissue engineering. *Drug Delivery*. 2020;27(1):1106–1114. doi:10.1080/10717544.2020.1797239
18. Hu Y, Zhao Z, Ehrich M, Fuhrman K, Zhang CJP. In vitro controlled release of antigen in dendritic cells using pH-sensitive liposome-polymeric hybrid nanoparticles. *Polymer*. 2015;80:171–179. doi:10.1016/j.polymer.2015.10.048
19. Yang Y, Chia H, Chung TS. Effect of preparation temperature on the characteristics and release profiles of PLGA microspheres containing protein fabricated by double-emulsion solvent extraction/evaporation method. *J Controlled Release*. 2000;69(1):81–96. doi:10.1016/s0168-3659(00)00291-1
20. Zhou Y, Zhu C, Wu Y, Zhang L, Tang JJC. Effective modulation of transforming growth factor-β1 expression through engineered microRNA-based plasmid-loaded nanospheres. *Cytotherapy*. 2015;17(3):320–329. doi:10.1016/j.jcyt.2014.09.004
21. Ghali A, El Malik E, Ibrahim A, Ismail G, Rashid M. Ureteric injuries: diagnosis, management, and outcome. *J Trauma*. 1999;46(1):150–158. doi:10.1097/00005373-199901000-00026
22. Engel O, Rink M, Fisch M. Management of iatrogenic ureteral injury and techniques for ureteral reconstruction. *Curr Opinion Urol*. 2015;25 (4):331–335. doi:10.1097/mou.0000000000000175
23. Ho D, Su S, Chang P, et al. Biodegradable Stent with mTOR Inhibitor-Eluting Reduces Progression of Ureteral Stricture. *Int J Mol Sci*. 2021;22 (11). doi:10.3390/ijms22115664.
24. Kram W, Rebl H, Wyrwa R, et al. Paclitaxel-coated stents to prevent hyperplastic proliferation of ureteral tissue: from in vitro to in vivo. *Urolithiasis*. 2020;48(1):47–56. doi:10.1007/s00240-018-1081-7
25. Lumiaho J, Heino A, Kauppinen T, et al. Drainage and antireflux characteristics of a biodegradable self-reinforced, self-expanding X-ray-positive poly-L,D-lactide spiral partial ureteral stent: an experimental study. *J Endourol*. 2007;21(12):1559–1564. doi:10.1089/end.2005.0085
26. Luo J, Zhao S, Wang J, et al. Bone marrow mesenchymal stem cells reduce ureteral stricture formation in a rat model via the paracrine effect of extracellular vesicles. *J Cell Mol Med*. 2018;22(9):4449–4459. doi:10.1111/jcmm.13744
27. Chung YC, Young TH. The exhibition of polyethylene imine/DNA coated with oligonucleotides for gene delivery. *Int Conf Chem*. 2010:119.
28. Maurer KJ, Rao VP, Ge Z, et al. T-cell function is critical for murine cholesterol gallstone formation. *Gastroenterology*. 2007;133(4):1304–1315. doi:10.1053/j.gastro.2007.07.005
29. Suen WLL. Size-dependent internalisation of folate-decorated nanoparticles via the pathways of clathrin and caveolae-mediated endocytosis in ARPE-19 cells. *Pharmacology*. 2014;66(4):564–573.
30. Anidjar M, Mongiat-Artus P, Brouland J, et al. Thermal radiofrequency induced porcine ureteral stricture: a convenient endourologic model. *J Urol*. 1999;161(1):298–303. doi:10.1097/00005392-199901000-00094
31. Yang Y, Zhou X, Gao H, Ji S, Wang C. The expression of epidermal growth factor and transforming growth factor-beta1 in the stenotic tissue of congenital pelvi-ureteric junction obstruction in children. *J Pediatric Surg*. 2003;38(11):1656–1660. doi:10.1016/s0022-3468(03)00577-3
32. Zhang D, Sun L, Xian W, et al. Low-dose paclitaxel ameliorates renal fibrosis in rat UUO model by inhibition of TGF-beta/Smad activity. *Lab Invest*. 2010;90(3):436–447. doi:10.1038/labinvest.2009.149